Journal of Molecular Modeling (2023) 29:198
https://doi.org/10.1007/s00894-023-05611-7

ORIGINAL PAPER

Ab initio study of water anchored in graphene pristine and vacancy-type defects

Mariana Zancan Tonel[1] · João Pedro Kleinubing Abal[2] · Solange Binotto Fagan[1] · Marcia Cristina Barbosa[2]

Received: 23 February 2023 / Accepted: 30 May 2023

Abstract

Context In this paper, we have addressed two issues that are relevant to the interaction of water in pristine and vacant graphene through first-principles calculations based on the Density Functional Theory (DFT). The results showed that for the interaction of pristine graphene with water, the DOWN configuration (with the hydrogen atoms facing downwards) was the most stable, presenting binding energies in the order of -13.62 kJ/mol at a distance of 2.375 Å in the TOP position. We also evaluated the interaction of water with two vacancy models, removing one carbon atom (Vac-1C) and four atoms (Vac-4C). In the Vac-1C system, the most favourable system was the DOWN configuration, with binding energies ranging from -20.60 kJ/mol to -18.41 kJ/mol in the TOP and UP positions, respectively. A different behaviour was observed for the interaction of water with Vac-4C; regardless of the configuration of the water, it is always more favourable for the interaction to occur through the vacancy centre, with binding energies between -13.28 kJ/mol and -20.49 kJ/mol. Thus, the results presented open perspectives for the technological development of nanomembranes as well as providing a better understanding of the wettability effects of graphene sheets, whether pristine or with defects.

Method We evaluated the interaction of pristine and vacant graphene with the water molecule, through calculations based on Density Functional Theory (DFT); implemented by the SIESTA program. The electronic, energetic, and structural properties were analyzed by solving self-consistent Kohn-Sham equations. In all calculations, a double ζ plus a polarized function (DZP) was used for the numerical baise set. Local Density Approximation (LDA) with the Perdew and Zunger (PZ) parameterisation along with a basis set superposition error (BSSE) correction were used to describe the exchange and correlation potential (Vxc). The water and isolated graphene structures were relaxed until the residual forces were less than 0.05 eV/Å^{-1} in all atomic coordinates.

Keywords Density functional theory · Carbon nanomaterials · Simulation approach · Water

Introduction

Water is a fascinating liquid. A material that occupies two-thirds of the surface of our planet and 70% of our body is certainly very important. Despite the abundance of water, the amount of freshwater on the planet corresponds to only 2.5% of the total volume of water. Today one in six people suffers from water scarcity and by the year 2025 one in two people will suffer from water stress [1]. One potential strategy to solve this problem is to understand the behaviour of water and, through its properties, look for economical ways to obtain more potable water [2–8].

Water exhibits more than 70 anomalies – thermodynamic, dynamic, and structural properties which allow it to differ from other materials [9]. These anomalous behaviours are responsible for the maintenance of life on the planet. In addition to

✉ Mariana Zancan Tonel
marianaztonel@gmail.com

João Pedro Kleinubing Abal
joaoabal@gmail.com

Solange Binotto Fagan
solange.fagan@gmail.com

Marcia Cristina Barbosa
marcia.barbosa@ufrgs.br

[1] Universidade Franciscana-UFN, PPGNANO - Postgraduate Program in Nanoscience, Rua dos Andradas, 1614, ZIP, Santa Maria, RS 97010-032, Brazil

[2] Universidade Federal do Rio Grande do Sul- UFRGS, Institute of Physics, Av. Bento Gonçalves, 9500 - Agronomia, ZIP, Porto Alegre, RS 91501-970, Brazil

Published online: 03 June 2023

its bulk anomalous properties, it was recently observed that water under confinement presented a fast flow, violating known hydrodynamic equations [9–13]. According to molecular dynamic simulations for classical atomistic models, this behaviour was attributed to the single line behaviour of water molecules under confinement in carbon nanotubes [14] and in graphene-based or other single layer materials nanopores [15].

Graphene is a carbon nanomaterial that has attracted great interest from the scientific community in recent years due to its electronic and structural characteristics [16, 17]. As it is an atom-thick material, it offers a wide range of applications such as in the electronics industry and in medicine [18–21]. Graphene is a two-dimensional (2D) material, that is, electrons are free to move in two directions and confined in one; its resultant large surface area makes graphene useful in a variety of applications [22–28]. For example, the adsorption capacity of graphene is mainly related to its surface area, and makes it suitable for the storage and capture of molecules for both biosensor and drug delivery applications [29, 30].

Membrane technology plays a crucial role in the chemical industry for molecular separations such as gas and liquid purification and greenhouse gas capture [24–26, 31–33]. In this sense, graphene and its large family of 2D materials are excellent platforms for designing ultra-thin nanoporous membranes for ultra-fast molecular separation, due to their atomic thickness, high surface area, mechanical durability, and industrial scalability [34–43]. It is currently being explored because of its direct impact on graphene-based devices such as water filtration membranes [44]; it can also be used as a model system for understanding the interaction between water and carbonaceous surfaces. However, relatively little is known about the behaviour of water diffusion in graphene and layered materials in general. In particular, it remains unknown how the large out-of-plane displacements exhibited by single layers of these materials might affect the movement of the adsorbed [44–46].

Although molecular dynamic simulations may be used to reveal the flow of water through nanopores in single layer materials, since the models employed to describe the layer and the water are classical, the specific way in which the water molecules approach the nanopore is unclear. A better knowledge of this process would be important in order to develop more accurate atomistic models.

In this paper, we have addressed two issues that are relevant to the interaction of water in pristine and vacant graphene through first-principles calculations based on the Density Functional Theory (DFT). We compared water-graphene energies with varying orientations and distances. The idea was to identify the lowest energy water-graphene and water-vacancy configurations. The other issue was the H-π interactions in defining the optimal water-graphene and water-vacancy configurations. This allowed us to understand the effect of these defects on the adsorption of water in pristine and vacant graphene.

The remainder of the paper is structured as follows. The methodology employed is presented in the next section. Then, the results are discussed and the conclusions are provided at the end of the manuscript.

Methodology

We studied the influence of the water molecule interaction with pristine graphene and with two vacancy versus distance models through density functional theory (DFT) [47, 48]; implemented in the SIESTA code (Spanish Initiative for Electronic Simulations of Thousands of Atoms) [49]. The electronic, energetic, and structural properties were analysed by solving self-consistent Kohn-Sham equations. In all calculations, a double ζ plus a polarised function (DZP) was used for the numerical base set. To describe the exchange and correlation potential (Vxc), we investigated through Local Density Approximation (LDA) with the Perdew and Zunger (PZ) parameterization [50] along with base set overlap error correction (BSSE corrected) [51]. This choice was justified in the first place by similar works in the literature [52–56] where LDA showed a better agreement for binding energies and binding distance values relative to experimental results. Secondly, LDA shows good agreement for weakly interacting systems, especially with the presence of π-stacking interactions in sp^2-type materials [57–61].

A grid cut of 200 Rydberg (Ry) was used to represent the electronic charge in real space. All systems studied had a neutral charge in their initial electronic configuration. The water and isolated graphene structures were relaxed until the residual forces were less than 0.05 $eV/Å^{-1}$ in all atomic coordinates. In addition, the pristine graphene studied showed 144 carbon atoms. Two vacancy models were also considered: vacancy-1C (Vac-1C), where one carbon atom was removed, and vacancy-4C (Vac-4C) where four carbon atoms were removed. Periodic boundary conditions were used in all simulations; the cells had dimensions of $25.94 \times 40.00 \times 14.98 Å^3$, also called the supercell method.

For the interaction energy calculations, the following equation was used with the BSSE [51] corrected for all calculations using the balance method:

$$E_b = E(A + B) - E\left(A_{ghost} + B\right) - E\left(A + B_{ghost}\right) \quad (1)$$

This correction was performed for the initial geometry of system AB and calculating the total energy of system A, considering the entire set of basis functions, where the set of basis functions B was in the position corresponding to system B, without the explicit presence of atoms. The same occurred in the calculation of system B. The system with negative binding energies implied attractive interactions.

Results

We initially evaluated pristine graphene (Gr), and analysed two situations of vacancy: removing one atom (Vac-1C) and four carbon atoms (Vac-4C) as illustrated in Fig. 1. The largest diameters were 2.60 and 4.60 Å for Vac-1C and Vac-4C, respectively. Vac-1C is experimentally stable [62–64], and has a spin polarization of 1.18 μB, according to theoretical studies [65, 66]. The Vac-4C evaluated in this work does not show polarization, according to previous studies [67–69] this type of vacancy defect in graphene is especially interesting because some models may not show spin polarization. The total electronic charge distributions were analysed, revealing that the charges were uniformly distributed over the carbon atoms in both pristine graphene and Vac-4C. In the case of Vac-1C, the charge plot was concentrated on the region where the carbon atom was removed.

Then, three main configurations were selected for water to interact with Gr/Vac-1C/Vac-4C): face to face (X-H_2O-FF) (Fig. 1(d)), T-shaped with oxygen facing down (X-H_2O-UP) (Fig. 1(e)), and T-shaped with the hydrogens facing down (X-H_2O-DOWN) (Fig. 1(f)). The interactions were evaluated on the carbon atom of the graphene lattice (TOP) and on the centre of the hexagon (vacancy) (HC). The interaction energy curves of these configurations were subsequently calculated as a function of the distance r between the graphene-molecule and the vacancy-molecule via DFT formalism with a basis set superposition error (BSSE) correction as indicated in Eq. 1.

Interactions of water with pristine graphene

Figure 2 shows the interaction of water with pristine graphene for three configurations Gr-H_2O-FF, Gr-H_2O-UP, and Gr-H_2O-DOWN, positioned in the centre of the hexagon (HC) and on the carbon atom of the lattice of graphene (TOP).

For Gr-H_2O-TOP-FF and Gr-H_2O-HC-FF, the water molecule interacted parallel to the graphene sheet. In these configurations, we observed that the most stable distance between the graphene sheet and the water was 3 Å. In addition, the energies of the two positions Gr-H_2O-TOP-FF and Gr-H_2O-HC-FF, were -8.88 kJ/mol and -10.35 kJ/mol, respectively. That is, there was an energy increase of 24% in the change from the TOP to the HC position.

In the case of the interaction of water in the UP position with the oxygen facing downwards, we observed that the water in the Gr-H_2O-TOP-UP configuration was slightly more energetic than in the Gr-H_2O-HC-UP configuration, with energies of -9.41 kJ/mol and -7.89 kJ/mol, respectively. These configurations presented a subtle change at the shortest distance; while in Gr-H_2O-TOP-UP the most stable distance was 3.00 Å, for the Gr-H_2O-TOP-UP configuration it was 2.75 Å.

Hamada [70] previously evaluated the water in the TOP position in the UP configuration, using different functionals implemented in SIESTA and obtaining energies

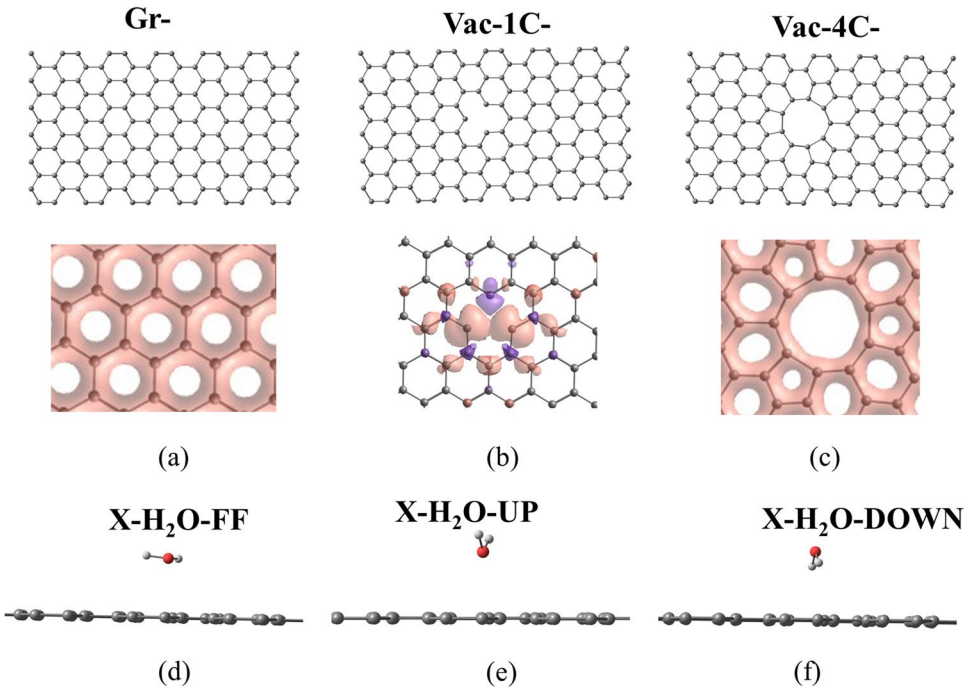

Fig. 1 **a** Pristine graphene, **b** vacancy with one missing carbon atom, **c** vacancy with four missing carbon atoms, with respective representations of the total charge (isosurface used in all molecules of 0.1 $e^-/Borh^3$, where e is the electronic charge and $Bohr^3$ (1 Bohr = 0.529 Å = 5.29×10^{-11} m) is the volume). Scheme of the studied configurations for the water interaction: **d** face to face (X-H_2O-FF), **e** T-shaped with oxygen facing downwards (X-H_2O-UP), and **f** T-shaped with the hydrogens facing down (X-H_2O-DOWN)

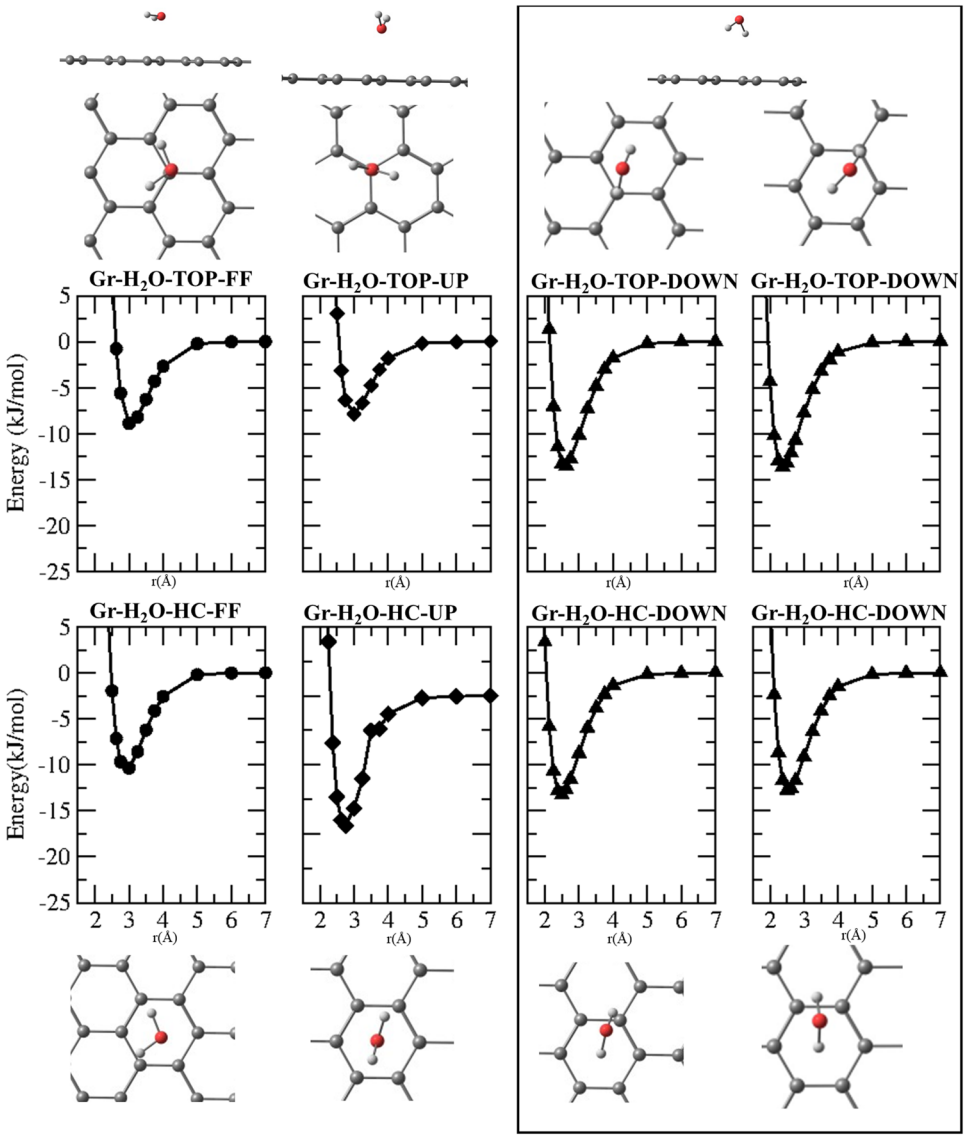

Fig. 2 Structural configurations and interaction energy curves computed for water interacting with pristine graphene (Gr-pristine): Gr-H_2O-(HC/TOP)-FF, Gr-H_2O-(HC/TOP)-UP, Gr-H_2O-(HC/TOP)-DOWN-1, Gr-H_2O-(HC/TOP)-DOWN-2

between -2.60 and -17.46 kJ/mol; the first energy was calculated with a GGA functional and the second with a van der Waals density functional (vdW-DF) [71]. These values are consistent with those presented in this work (-7.89 kJ/mol), since an LDA functional [50] and basis set superposition error (BSSE) correction [51] were used here.

The most stable configuration of water interacting with pristine graphene was DOWN (with the hydrogens facing downwards). In this position, we tested different angulations of entry of the H_2O molecule but did not observe significant changes in the energetic values over more stable distances as shown in Fig. 2. Comparing the interactions in Gr-H_2O-TOP-DOWN-1 with Gr-H_2O-TOP-DOWN-2, the lowest energies and minima were -13.50 kJ/mol (2.625 Å) and -13.62 kJ/mol (2.375 Å) for the two configurations, respectively. In addition, Gr-H_2O-HC-DOWN-1 and Gr-H_2O-HC-DOWN-2 presented the lowest energies at 2.50 Å with -13.27 kJ/mol and -12.80 kJ/ mol, respectively.

Voloshina and collaborators [72] previously evaluated the interaction of water with pristine graphene in the Gr-H_2O-HC-DOWN and Gr-H_2O-TOP-DOWN positions, yielding energies of -13.02 kJ/mol (3.06 Å) and -10.61 kJ/mol (3.06 Å), respectively. These values are very close to those presented here, although the authors adopted a different methodology, CCSD(T) [73–75]. Using a similar methodology (LDA) without a BSSE correction, Ma and colleagues obtained an energy of 14.5 kJ/mol for the water adsorbed on graphene in the DOWN position [76].

Silvestrelli and Ambrosetti (2014) [77] evaluated the interaction of water in graphene through DFT calculations with different functionals. The most energetic system of water interacting with graphene, Silvestrelli and Ambrosetti [77] obtained an energy of -13.50 kJ/mol using the LDA

functional. Experimental studies, on the other hand, have shown that the binding energy of water in graphite was in the order of -15.05 kJ/mol [78].

A different behaviour of water was observed in the DOWN configuration than in the other configurations; in this case, the TOP position was more energetic than the HC one. This was due to an approximation between the two atoms of hydrogen (H_2O) and carbon (Gr). In addition, we observed that the point of greatest interaction between water and Gr-pristine occurs at a shorter distance, compared to the other configurations (Gr-H2O-HC-UP/Gr-H2O-TOP-UP and Gr-H2O-HC-FF /Gr-H2O-TOP-FF).

In general, previous studies [79] employing first principles calculations using different types of functionals for the van-der-Waals interactions [70, 76] have shown that configurations with one or two OH bonds of the water molecule pointing down to the graphene sheet were energetically favoured, having similar adsorption energies and therefore similar stabilities. The adsorption energies and geometries were in good agreement with data reported in previous works [70–76]: The adsorption energies were ~2.89 kJ/mol for PBE, ~13.02 kJ/mol for DFT-D2, ~14.18 kJ/mol for vdW-DF, and ~14.66 eV for optPBE-vdW.

Interactions of water with vacancy defect-bearing graphene

Figures 3 and 4 illustrate the interaction of water with graphene with two types of vacancy defects. In the first case, shown in Fig. 3, one carbon atom was removed from the graphene hexagonal network (Vac-1C) and in the second, illustrated in Fig. 4, four carbon atoms were removed (Vac-4C).

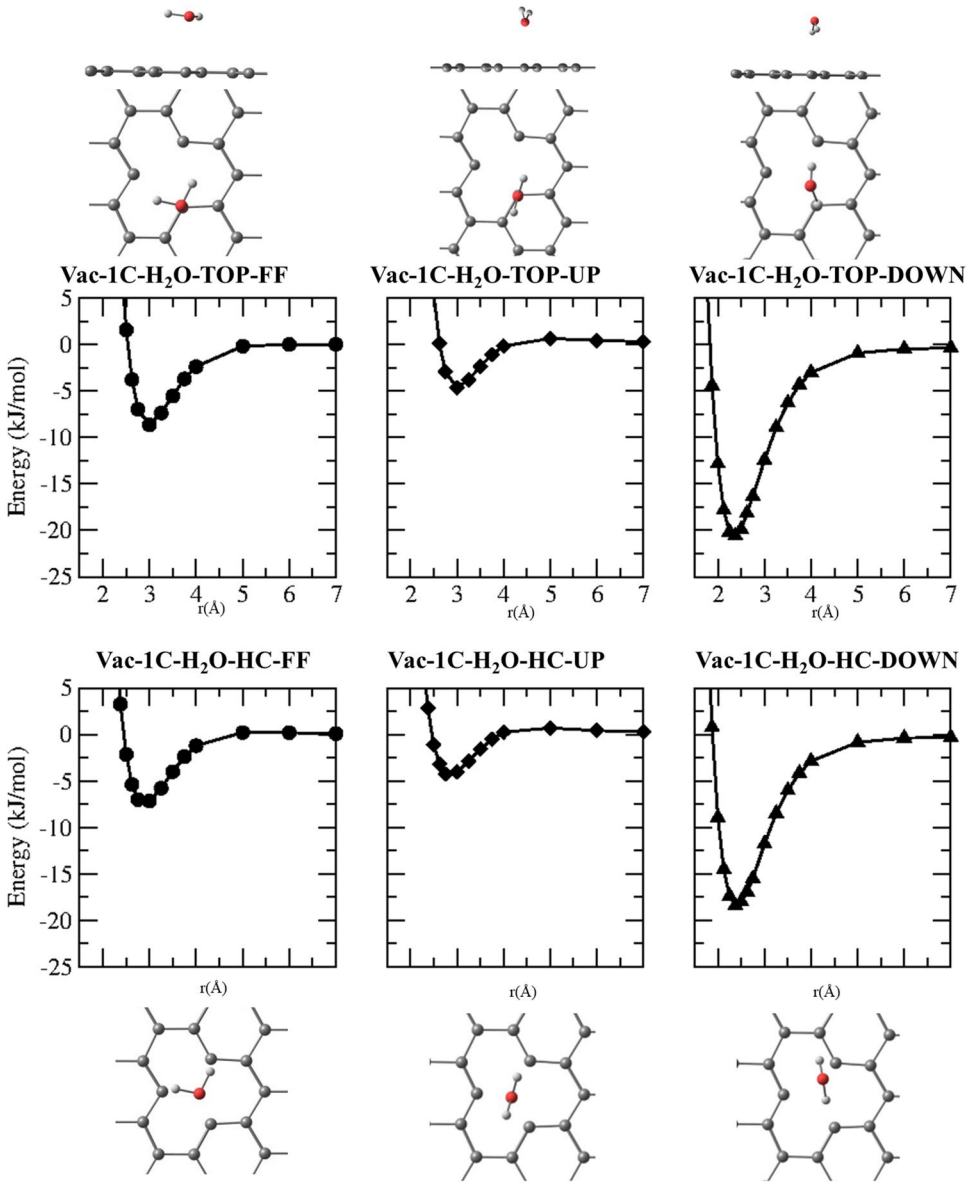

Fig. 3 Structural configurations and interaction energy curves computed for water interacting with graphene containing a vacancy (one missing carbon atom): Vac-1C-H_2O-(HC/TOP)-FF, Vac-1C-H_2O-(HC/TOP)-UP, Vac-1C-H_2O-(HC/TOP)-DOWN

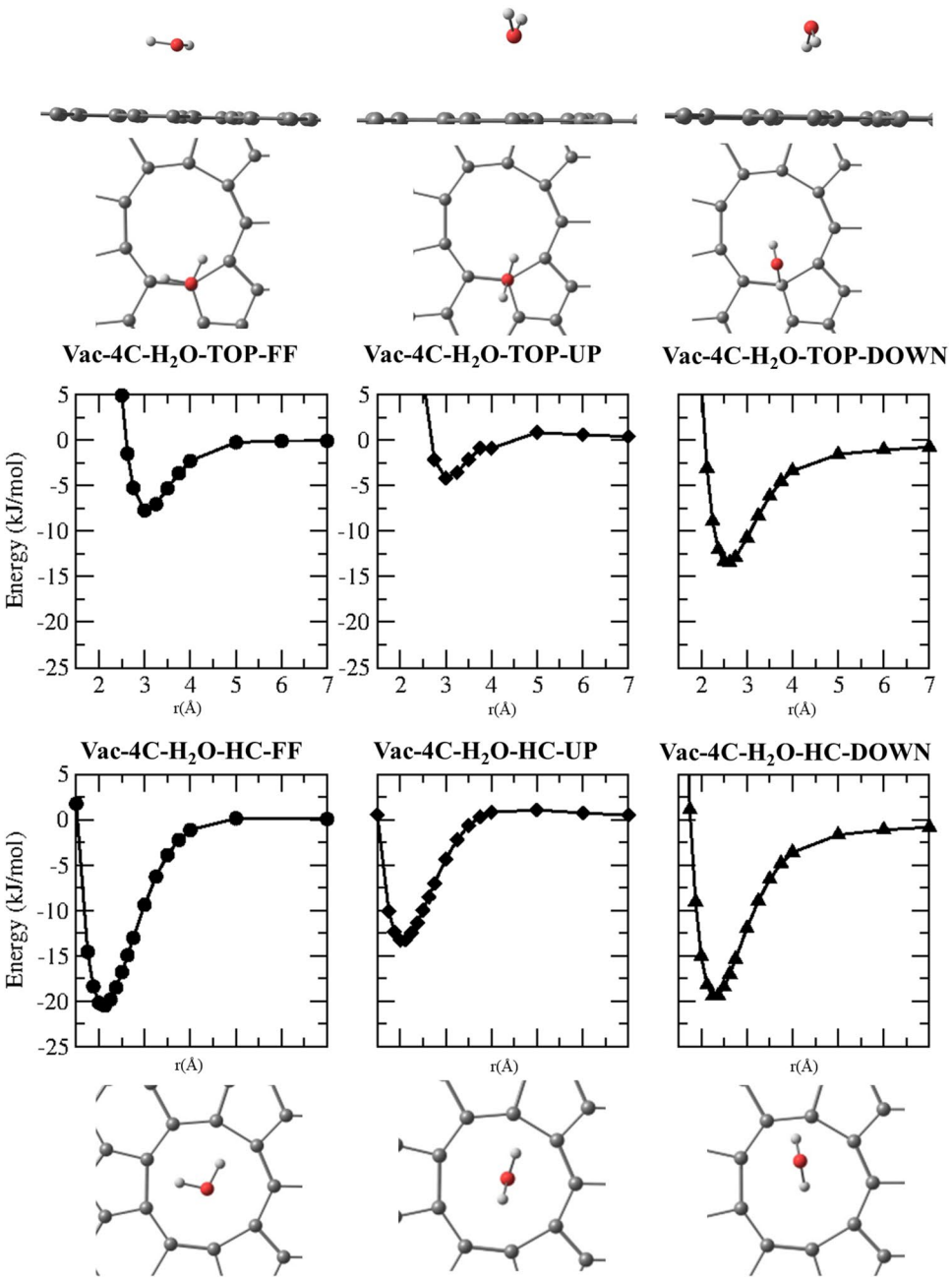

Fig. 4 Structural configurations and interaction energy curves computed for water interacting with graphene containing a vacancy (four missing carbon atoms): Vac-4C-H_2O-(HC/TOP)-FF, Vac-4C-H_2O-(HC/TOP)-UP, Vac-4C-H_2O-(HC/TOP)-DOWN

The structures were then relaxed until the convergence criteria described in the methodology section were reached. The average diameters for Vac-1C and Vac-4C were 2.60 and 4.60 Å, respectively. The same scheme as described earlier was used to investigate the interactions with water: face to face (Vac-1C/Vac-4C)-H2O-FF, T-shaped with oxygen facing down (Vac-1C/Vac-4C)-H2O-UP, and T-shaped with the hydrogens facing down (Vac-1C/Vac-4C)-H2O-DOWN.

Figure 3 shows the energy curves of the interaction of water with Vac-1C. The first configuration studied was Vac-1C-H_2O-TOP-FF in which the highest binding energy was -8.65 kJ/mol, . In the case of Vac-1C-H_2O-HC-FF, where the water molecule was arranged in the centre of the vacancy, the energy was -7.15 kJ/mol. In both cases, the best stability point was at a distance of r = 3.00 Å.

When arranged in the UP position (oxygen facing downwards), the water on the graphene sheet did not show significant changes in energy in the TOP or HC position, with values of 4.64 and -4.26 kJ/mol, respectively. In this case, there was a small shift in the distance from the energy minimum, from r = 3.00 Å (Vac-1C-H_2O-TOP-UP) to r = 2.75 Å.

The highest values of binding energy (lowest energy) were obtained when the water was arranged with the hydrogens facing downwards (DOWN). For the

Vac-1C-H_2O-TOP-DOWN configuration the minimum energy was -20.60 kJ/mol, and for Vac-1C-H_2O-HC-DOWN an energy of -18.41 kJ/mol was obtained. In both cases the minimum energy was at a distance r = 2.375 Å.

Figure 4 shows the configurations and interaction energy curves calculated for the interactions of water and Vac-4C, in kJ/mol units.

When the water molecule was arranged in a face-to-face configuration on the Vac-4C in the TOP position, a minimum interaction energy of -7.74 kJ/mol was obtained and the minimum energy distance was r = 3.00 Å. The same configuration interacting in the HC position of the vacancy occurred with an increase of 260% of energy, becoming -20.49 kJ/mol; the distance of greater stability also decreased to r = 2.125 Å.

In the UP configuration with the oxygen facing downwards, the interaction at the TOP position had a minimum energy of -4.19 kJ/mol. Changing to the HC position increased it to -13.28 kJ/mol, that is, the energy increased by more than 300% relative to the TOP position. A modification of the distances also occurred; while in Vac-4C-H_2O-UP-TOP r = 3.00 Å, the equilibrium distance for Vac-4C-H_2O-UP-HC was r = 2.00 Å.

In the DOWN position, where the water was arranged with the hydrogen atoms facing the Vac-4C, the Vac-4C-H_2O-DOWN-TOP configuration had an energy minimum of -13.47 kJ/mol with r = 2.625 Å. In the Vac-4C-H_2O-DOWN-HC configuration, the minimum energy occurred with r = 2.25 Å, and in this case, the minimum energy was -19.44 kJ/mol.

The interactions of the water molecules with Vac-4C were very similar between the different configurations in the HC position. When water interacted with Vac-4C in the TOP position, the most stable distances and energies were similar or inferior to the values of Gr-pristine or Vac-1C. However, it was energetically more favorable for water to interact with Vac-4C in the HC position regardless of the studied configuration, and in these cases a greater proximity of the water molecule to the vacancy was observed.

The configuration that showed the best stability was Vac-4C-HC-FF with an energy of -20.49 kJ/mol. According to Lim and Kim [41], the face-to-face configuration is the most stable because as the H_2O molecule gradually flattens and approaches a pore, its hydrogen atoms will directly bond with two carbon atoms within the vacancy. This planar hydrogen bond geometry is possible because the folded geometry of the H_2O molecule is uniquely compatible with vacancy symmetry. Our observations also validate the conclusions of previous molecular dynamics studies which suggest that a greater pore hydrophilicity, i.e., improved hydrogen bonding interaction, results in an easier water permeation [79–85]. On a similar note, it would be important to consider permeation in the presence of multiple H_2O molecules. For example, the hydrogen bonding interaction between two H_2O molecules across a pore has been shown to be capable of reducing reduce the permeation energy barrier [86, 87].

The interactions of Gr, Vac-1C, and Vac-4C with water in the face-to-face (FF) configuration exhibited a similar behaviour, except for Vac-4C-FF-HC. In most cases, a greater stabilisation occurred at a distance of r = 3 Å and the binding energies ranged from -7.15 to -10.34 kJ/mol. In the Vac-4C-FF-HC configuration, which was the exception, an energy increase of more than 100% was observed in relation to the energies of the others, and stabilisation occurred at r = 2.125 Å. This indicates that the size of the vacancy directly influenced the absorption.

We show here energy versus distance curves for the interaction of water in pristine graphene and with vacancy-type defects. However, here we show for the first time that there is a small orientational dependence on the adsorption energy of the water monomer, but rather a dependence on the position and size of the vacancy. These electronic structure approaches are becoming a robust and reliable tool and have the prospect of being routinely applied to surface adsorption problems [88]. Thus, the results presented open perspectives for the technological development of nanomembranes, as well as the understanding of water diffusion through pristine graphene and with vacancy-type defects.

Conclusions

We have evaluated the interaction of a water monomer with a pristine graphene sheet and with two vacancy models – removing one carbon atom (Vac-1C) or four atoms (Vac-4C) from the graphene lattice. Different orientations of water resulted in relatively different interactions with the graphene layer, but the binding energies were ultimately very similar. However, regardless of the configuration, the water monomer preferentially interacted with graphene through the centre of the greatest vacancy (Vac-4C), indicating that graphene with vacancies is favorable to be used with nanomembranes.

Our results suggest that water was preferentially arranged at the graphene surface in a Vac-1C-H_2O-TOP-DOWN conformation (-20.60 kJ/mol) at r = 2.375 Å. The energy given by the minimum was larger than the thermal energy and that of the hydrogen bond network, indicating that water will not flow through a pore in a thermal system. This result is consistent with those of atomistic simulations which indicate that water does not flow through pores below a threshold.

Acknowledgement The authors acknowledge CENAPAD-SP (Centro Nacional de Processamento de Alto Desempenho em São Paulo), UFN (Universidade Franciscana) and UFRGS (Universidade Federal do Rio Grande do Sul) for computer time and the Brazilian agencies CNPQ and CAPES for financial support.

Authors' contributions Mariana Zancan Tonel, João Pedro Kleinubing Abal, Solange Binotto Fagan, Marcia Cristina Bernardes Barbosa contributed to the design of the study, carried out the simulations and wrote the manuscript. Mariana Zancan Tonel, João Pedro Kleinubing Abal, Solange Binotto Fagan, Marcia Cristina Bernardes Barbosa analyzed the data with constructive discussions. Marcia Cristina Bernardes Barbosa supervised the research.

Funding This study is funded by Coordenação de Aperfeiçoamento de Pessoal de Nível Superior, CAPES and National Council for Scientific and Technological Development, CNPq (scholarship).

Data availability N/A

Declarations

Ethics approval N/A

Consent to participate The manuscript is approved by all authors for publication.

Consent for publication The consent for publication was obtained from all participants.

Conflicts of interest The authors declare that they have no competing interests.

References

1. (2018) Water scarcity | International Decade for Action "Water for Life" 2005-2015. http://www.un.org/waterforlifedecade/scarcity.shtml. Accessed 23 Oct 2018
2. Barbosa RD, Barbosa MC (2015) Hydration shell of the TS-Kappa protein: higher density than bulk water. Physica A: Stat Mech Appl 439:48–58. https://doi.org/10.1016/j.physa.2015.07.026
3. Köhler MH, Barbosa RC, da Silva LB, Barbosa MC (2017) Role of the hydrophobic and hydrophilic sites in the dynamic crossover of the protein-hydration water. Physica A: Stat Mech Appl 468:733–739. https://doi.org/10.1016/j.physa.2016.11.127
4. Köhler MH, Bordin JR, da Silva LB, Barbosa MC (2018) Structure and dynamics of water inside hydrophobic and hydrophilic nanotubes. Physica A: Stat Mech Appl 490:331–337. https://doi.org/10.1016/j.physa.2017.08.030
5. Köhler MH, da Silva LB (2016) Size effects and the role of density on the viscosity of water confined in carbon nanotubes. Chem Phys Lett 645:38–41. https://doi.org/10.1016/j.cplett.2015.12.020
6. Krott LB, Barbosa MC (2014) Model of waterlike fluid under confinement for hydrophobic and hydrophilic particle-plate interaction potentials. Phys Rev E 89:012110. https://doi.org/10.1103/PhysRevE.89.012110
7. Lehnert U, Réat V, Weik M et al (1998) Thermal motions in bacteriorhodopsin at different hydration levels studied by neutron scattering: correlation with kinetics and light-induced conformational changes. Biophys J 75:1945–1952. https://doi.org/10.1016/S0006-3495(98)77635-0
8. Tsai AM, Neumann DA, Bell LN (2000) Molecular dynamics of solid-state lysozyme as affected by glycerol and water: a neutron scattering study. Biophys J 79:2728–2732. https://doi.org/10.1016/S0006-3495(00)76511-8
9. Chaplin M https://water.lsbu.ac.uk/water/water_structure_science.html
10. Majumder M, Chopra N, Andrews R, Hinds BJ (2005) Enhanced flow in carbon nanotubes. Nature 438:44–44. https://doi.org/10.1038/438044a
11. Holt JK, Park HG, Wang Y et al (2006) Fast mass transport through sub-2-nanometer carbon nanotubes. Science 312:1034–1037. https://doi.org/10.1126/science.1126298
12. Qin X, Yuan Q, Zhao Y et al (2011) Measurement of the rate of water translocation through carbon nanotubes. Nano Lett 11:2173–2177. https://doi.org/10.1021/nl200843g
13. Hummer G, Rasaiah JC, Noworyta JP (2001) Water conduction through the hydrophobic channel of a carbon nanotube. Nature 414:188–190. https://doi.org/10.1038/35102535
14. Bordin JR, Diehl A, Barbosa MC (2013) Relation between flow enhancement factor and structure for core-softened fluids inside nanotubes. J Phys Chem B 117:7047–7056. https://doi.org/10.1021/jp402141f
15. Abal JPK, Bordin JR, Barbosa MC (2020) Salt parameterization can drastically affect the results from classical atomistic simulations of water desalination by MoS_2 nanopores. Phys Chem Chem Phys 22:11053–11061. https://doi.org/10.1039/D0CP00484G
16. Castro Neto AH, Guinea F, Peres NMR et al (2009) The electronic properties of graphene. Rev Mod Phys 81:109–162. https://doi.org/10.1103/RevModPhys.81.109
17. Rao CNR, Sood AK, Subrahmanyam KS, Govindaraj A (2009) Graphene: the new two-dimensional nanomaterial. Angew Chem Int Ed 48:7752–7777. https://doi.org/10.1002/anie.200901678
18. Abergel DSL, Apalkov V, Berashevich J et al (2010) Properties of graphene: a theoretical perspective. Adv Phys 59:261–482. https://doi.org/10.1080/00018732.2010.487978
19. Geim AK, Novoselov KS (2007) The rise of graphene. Nature Mater 6:183–191. https://doi.org/10.1038/nmat1849
20. Robinson JT, Perkins FK, Snow ES et al (2008) Reduced graphene oxide molecular sensors. Nano Lett 8:3137–3140. https://doi.org/10.1021/nl8013007
21. Rodríguez SJ, Makinistian L, Albanesi EA (2017) Graphene for amino acid biosensing: theoretical study of the electronic transport. Appl Surface Sci 419:540–545. https://doi.org/10.1016/j.apsusc.2017.05.031
22. Berman D, Deshmukh SA, Sankaranarayanan SKRS et al (2015) Macroscale superlubricity enabled by graphene nanoscroll formation. Science 348:1118–1122. https://doi.org/10.1126/science.1262024
23. Gan T, Hu S (2011) Electrochemical sensors based on graphene materials. Microchim Acta 175:1–19. https://doi.org/10.1007/s00604-011-0639-7
24. Garaj S, Hubbard W, Reina A et al (2010) Graphene as a subnanometre trans-electrode membrane. Nature 467:190–193. https://doi.org/10.1038/nature09379
25. Kim HW, Yoon HW, Yoon S-M et al (2013) Selective gas transport through few-layered graphene and graphene oxide membranes. Science 342:91–95. https://doi.org/10.1126/science.1236098
26. Miller JR, Outlaw RA, Holloway BC (2010) Graphene double-layer capacitor with ac line-filtering performance. Science 329:1637–1639. https://doi.org/10.1126/science.1194372
27. Son Y-W, Cohen ML, Louie SG (2006) Half-metallic graphene nanoribbons. Nature 444:347–349. https://doi.org/10.1038/nature05180
28. Zhong Y, Zhen Z, Zhu H (2017) Graphene: Fundamental research and potential applications. Flat Chem 4:20–32. https://doi.org/10.1016/j.flatc.2017.06.008
29. Goenka S, Sant V, Sant S (2014) Graphene-based nanomaterials for drug delivery and tissue engineering. J Controlled Release 173:75–88. https://doi.org/10.1016/j.jconrel.2013.10.017
30. Urbas K, Aleksandrzak M, Jedrzejczak M et al (2014) Chemical and magnetic functionalization of graphene oxide as a route to enhance its biocompatibility. Nanoscale Res Lett 9:656. https://doi.org/10.1186/1556-276X-9-656
31. Defontaine G, Barichard A, Letaief S et al (2010) Nanoporous polymer – clay hybrid membranes for gas separation. J Colloid Int Sci 343:622–627. https://doi.org/10.1016/j.jcis.2009.11.048

32. Furmaniak S, Kowalczyk P, Terzyk AP et al (2013) Synergetic effect of carbon nanopore size and surface oxidation on CO2 capture from CO2/CH4 mixtures. J Colloid Inter Sci 397:144–153. https://doi.org/10.1016/j.jcis.2013.01.044
33. Lin L, Zhang Y, Li H (2010) Pervaporation and sorption behavior of zeolite-filled polyethylene glycol hybrid membranes for the removal of thiophene species. J Colloid Inter Sci 350:355–360. https://doi.org/10.1016/j.jcis.2010.06.031
34. Algara-Siller G, Lehtinen O, Wang FC et al (2015) Square ice in graphene nanocapillaries. Nature 519:443–445. https://doi.org/10.1038/nature14295
35. Celebi K, Buchheim J, Wyss RM et al (2014) Ultimate permeation across atomically thin porous graphene. Science 344:289–292. https://doi.org/10.1126/science.1249097
36. Cheng M, Wang D, Sun Z et al (2014) A route toward digital manipulation of water nanodroplets on surfaces. ACS Nano 8:3955–3960. https://doi.org/10.1021/nn500873q
37. Cicero G, Grossman JC, Schwegler E et al (2008) Water confined in nanotubes and between graphene sheets: a first principle study. J Am Chem Soc 130:1871–1878. https://doi.org/10.1021/ja074418+
38. Feng X, Maier S, Salmeron M (2012) Water splits epitaxial graphene and intercalates. J Am Chem Soc 134:5662–5668. https://doi.org/10.1021/ja3003809
39. Kim W, Nair S (2013) Membranes from nanoporous 1d and 2d materials: a review of opportunities, developments, and challenges. Chem Eng Sci 104:908–924. https://doi.org/10.1016/j.ces.2013.09.047
40. Li Z, Wang Y, Kozbial A et al (2013) Effect of airborne contaminants on the wettability of supported graphene and graphite. Nature Mater 12:925–931. https://doi.org/10.1038/nmat3709
41. Lim JS, Kim G (2019) First-principles modeling of water permeation through periodically porous graphene derivatives. J Colloid Inter Sci 538:367–376. https://doi.org/10.1016/j.jcis.2018.11.106
42. Ying Y, Yang Y, Ying W, Peng X (2016) Two-dimensional materials for novel liquid separation membranes. Nanotechnology 27:332001. https://doi.org/10.1088/0957-4484/27/33/332001
43. Zheng Z, Grünker R, Feng X (2016) Synthetic two-dimensional materials: a new paradigm of membranes for ultimate separation. Adv Mater 28:6529–6545. https://doi.org/10.1002/adma.201506237
44. Nair RR, Wu HA, Jayaram PN et al (2012) Unimpeded permeation of water through helium-leak–tight graphene-based membranes. Science 335:442–444. https://doi.org/10.1126/science.1211694
45. Fasolino A, Los JH, Katsnelson MI (2007) Intrinsic ripples in graphene. Nature Mater 6:858–861. https://doi.org/10.1038/nmat2011
46. Los JH, Katsnelson MI, Yazyev OV et al (2009) Scaling properties of flexible membranes from atomistic simulations: application to graphene. Phys Rev B 80:121405. https://doi.org/10.1103/PhysRevB.80.121405
47. Hohenberg P, Kohn W (1964) Inhomogeneous electron gas. Phys Rev 136:B864–B871. https://doi.org/10.1103/PhysRev.136.B864
48. Kohn W, Sham LJ (1965) Self-consistent equations including exchange and correlation effects. Phys Rev 140:A1133–A1138. https://doi.org/10.1103/PhysRev.140.A1133
49. Soler JM, Artacho E, Gale JD et al (2002) The SIESTA method for *ab initio* order- *N* materials simulation. J Phys: Condens Matter 14:2745–2779. https://doi.org/10.1088/0953-8984/14/11/302
50. Perdew JP, Zunger A (1981) Self-interaction correction to density-functional approximations for many-electron systems. Phys Rev B 23:5048–5079. https://doi.org/10.1103/PhysRevB.23.5048
51. Boys SF, Bernardi F (1970) The calculation of small molecular interactions by the differences of separate total energies. Some procedures with reduced errors. Mol Phys 19:553–566. https://doi.org/10.1080/00268977000101561
52. de Moraes EE, Tonel MZ, Fagan SB, Barbosa MC (2019) Density functional theory study of π-aromatic interaction of benzene, phenol, catechol, dopamine isolated dimers and adsorbed on graphene surface. J Mol Model 25:302. https://doi.org/10.1007/s00894-019-4185-2
53. Hernández JMG, Anota EC, de la Cruz MTR et al (2012) First principles studies of the graphene-phenol interactions. J Mol Model 18:3857–3866. https://doi.org/10.1007/s00894-012-1382-7
54. Jauris IM, Matos CF, Saucier C et al (2016) Adsorption of sodium diclofenac on graphene: a combined experimental and theoretical study. Phys Chem Chem Phys 18:1526–1536. https://doi.org/10.1039/C5CP05940B
55. Jauris IM, Fagan SB, Adebayo MA, Machado FM (2016) Adsorption of acridine orange and methylene blue synthetic dyes and anthracene on single wall carbon nanotubes: a first principle approach. Comput Theor Chem 1076:42–50. https://doi.org/10.1016/j.comptc.2015.11.021
56. Machado FM, Carmalin SA, Lima EC et al (2016) Adsorption of alizarin red s dye by carbon nanotubes: an experimental and theoretical investigation. J Phys Chem C 120:18296–18306. https://doi.org/10.1021/acs.jpcc.6b03884
57. Arrigoni M, Madsen GKH (2019) Comparing the performance of LDA and GGA functionals in predicting the lattice thermal conductivity of III-V semiconductor materials in the zincblende structure: the cases of AlAs and BAs. Comput Mater Sci 156:354–360. https://doi.org/10.1016/j.commatsci.2018.10.005
58. Cresti A, Lopez-Bezanilla A, Ordejón P, Roche S (2011) Oxygen surface functionalization of graphene nanoribbons for transport gap engineering. ACS Nano 5:9271–9277. https://doi.org/10.1021/nn203573y
59. Li B, Ou P, Wei Y et al (2018) Polycyclic aromatic hydrocarbons adsorption onto graphene: a DFT and AIMD Study. Materials 11:726. https://doi.org/10.3390/ma11050726
60. Tournus F, Charlier J-C (2005) *Ab initio* study of benzene adsorption on carbon nanotubes. Phys Rev B 71:165421. https://doi.org/10.1103/PhysRevB.71.165421
61. Tournus F, Latil S, Heggie MI, Charlier J-C (2005) π -stacking interaction between carbon nanotubes and organic molecules. Phys Rev B 72:075431. https://doi.org/10.1103/PhysRevB.72.075431
62. Meyer JC, Kisielowski C, Erni R et al (2008) Direct imaging of lattice atoms and topological defects in graphene membranes. Nano Lett 8:3582–3586. https://doi.org/10.1021/nl801386m
63. Gass MH, Bangert U, Bleloch AL et al (2008) Free-standing graphene at atomic resolution. Nature Nanotech 3:676–681. https://doi.org/10.1038/nnano.2008.280
64. Ugeda MM, Brihuega I, Guinea F, Gómez-Rodríguez JM (2010) Missing atom as a source of carbon magnetism. Phys Rev Lett 104:096804. https://doi.org/10.1103/PhysRevLett.104.096804
65. Wu Y, Hu Y, Xue L et al (2018) Magnetism of a relaxed single atom vacancy in graphene. Physica B: Condensed Matter 534:184–188. https://doi.org/10.1016/j.physb.2018.01.040
66. Valencia AM, Caldas MJ (2017) Single vacancy defect in graphene: Insights into its magnetic properties from theoretical modeling. Phys Rev B 96:125431. https://doi.org/10.1103/PhysRevB.96.125431
67. Bao Z, Shi J, Yang M et al (2011) Magnetism induced by D3-symmetry tetra-vacancy defects in graphene. Chem Phys Lett 510:246–251. https://doi.org/10.1016/j.cplett.2011.05.056
68. Dai XQ, Zhao JH, Xie MH et al (2011) First-principle study of magnetism induced by vacancies in graphene. Eur Phys J B 80:343–349. https://doi.org/10.1140/epjb/e2011-10955-x
69. Wang C, Wang Z, Zhang S et al (2023) Ab initio investigation of the adsorption of co2 molecules on defect sites of graphene

surfaces: role of local vacancy Structures. Materials 16:981. https://doi.org/10.3390/ma16030981
70. Hamada I (2012) Adsorption of water on graphene: A van der Waals density functional study. Phys Rev B 86:195436. https://doi.org/10.1103/PhysRevB.86.195436
71. Dion M, Rydberg H, Schröder E et al (2004) Van der waals density functional for general geometries. Phys Rev Lett 92:246401. https://doi.org/10.1103/PhysRevLett.92.246401
72. Voloshina E, Usvyat D, Schütz M et al (2011) On the physisorption of water on graphene: a CCSD(T) study. Phys Chem Chem Phys 13:12041. https://doi.org/10.1039/c1cp20609e
73. Deegan MJO, Knowles PJ (1994) Perturbative corrections to account for triple excitations in closed and open shell coupled cluster theories. Chem Phys Lett 227:321–326. https://doi.org/10.1016/0009-2614(94)00815-9
74. Hampel C, Werner H (1996) Local treatment of electron correlation in coupled cluster theory. J Chem Phys 104:6286–6297. https://doi.org/10.1063/1.471289
75. Watts JD, Gauss J, Bartlett RJ (1993) Coupled-cluster methods with noniterative triple excitations for restricted open-shell Hartree–Fock and other general single determinant reference functions. Energies and analytical gradients. J Chem Phys 98:8718–8733. https://doi.org/10.1063/1.464480
76. Ma J, Michaelides A, Alfè D et al (2011) Adsorption and diffusion of water on graphene from first principles. Phys Rev B 84:033402. https://doi.org/10.1103/PhysRevB.84.033402
77. Silvestrelli PL, Ambrosetti A (2014) Including screening in van der waals corrected density functional theory calculations: the case of atoms and small molecules physisorbed on graphene. J Chem Phys 140:124107. https://doi.org/10.1063/1.4869330
78. Coughlin RW (1971) Chemistry and physics of carbon. Carbon 9:528–531. https://doi.org/10.1016/0008-6223(71)90037-6
79. Yang Y, Liu F, Kawazoe Y (2019) Adsorption of water on fluorinated graphene. J Phys Chem Solids 124:54–59. https://doi.org/10.1016/j.jpcs.2018.08.030
80. Cohen-Tanugi D, Grossman JC (2012) Water desalination across nanoporous graphene. Nano Lett 12:3602–3608. https://doi.org/10.1021/nl3012853
81. Kieu HT, Liu B, Zhou K, Law AW-K (2017) Pressure-driven water permeation through multilayer graphene nanosheets: pressure-driven water permeation through graphene nanosheets. Phys Status Solidi B 254:1700074. https://doi.org/10.1002/pssb.201700074
82. Shahbabaei M, Tang D, Kim D (2017) Simulation insight into water transport mechanisms through multilayer graphene-based membrane. Comput Mater Sci 128:87–97. https://doi.org/10.1016/j.commatsci.2016.10.044
83. Shi Q, He Z, Gupta KM et al (2017) Efficient ethanol/water separation via functionalized nanoporous graphene membranes: insights from molecular dynamics study. J Mater Sci 52:173–184. https://doi.org/10.1007/s10853-016-0319-4
84. Wang Y, He Z, Gupta KM et al (2017) Molecular dynamics study on water desalination through functionalized nanoporous graphene. Carbon 116:120–127. https://doi.org/10.1016/j.carbon.2017.01.099
85. Yu T, Bai L, Xu Z, Yang X (2018) Molecular simulation of permeation behaviour of ethanol/water molecules with single-layer graphene oxide membranes. Molecular Simulation 44:840–849. https://doi.org/10.1080/08927022.2018.1464161
86. Ambrosetti A, Silvestrelli PL (2014) Gas separation in nanoporous graphene from first principle calculations. J Phys Chem C 118:19172–19179. https://doi.org/10.1021/jp504914u
87. Bartolomei M, Carmona-Novillo E, Hernández MI et al (2014) Penetration barrier of water through graphynes' pores: first-principles predictions and force field optimization. J Phys Chem Lett 5:751–755. https://doi.org/10.1021/jz4026563
88. Brandenburg JG, Zen A, Fitzner M et al (2019) Physisorption of water on graphene: subchemical accuracy from many-body electronic structure methods. J Phys Chem Lett 10:358–368. https://doi.org/10.1021/acs.jpclett.8b03679